Finite-temperature band theory of ferromagnetic-antiferromagnetic interfaces including exchange anisotropy

Hideo Hasegawa
IBM Research Division, Almaden Research Center, San Jose, California 95120-6099
and The Institute for Solid State Physics, The University of Tokyo, 7-22-1 Roppongi, Minato-ku, Tokyo 106, Japan*

Frank Herman
IBM Research Division, Almaden Research Center, San Jose, California 95120-6099
(Received 8 January 1988)

In order to gain a microscopic understanding of ferromagnetic-antiferromagnetic (F-AF) interfaces, we have calculated the finite-temperature properties of Co/Cr superlattices using a tight-binding band-structure model and the single-site spin-fluctuation theory proposed independently by Hubbard and Hasegawa. The distribution of local magnetic moments on Co and Cr layers was determined as a function of the temperature in an eight-layer (3 Co + 5 Cr) bcc superlattice with [001] interfaces. Using these results, we performed a calculation of the temperature dependence of the exchange anisotropy constant, $\mathcal{J}$, and the effective exchange field, H_{ex}, associated with F-AF interfaces. The peculiar temperature dependence of $\mathcal{J}$ and H_{ex} arises from the nearest-neighbor interlayer exchange interaction across the F-AF interface. This interfacial exchange interaction is much smaller than the corresponding interactions in the F and AF regions. Our results account quite well for the general magnetic behavior observed in many F-AF interface systems.

I. INTRODUCTION

Since the discovery of exchange anisotropy by Meiklejohn and Bean in Co-CoO alloys,[1] ferromagnetic-antiferromagnetic (F-AF) interface systems have attracted both scientific and technological interest. Many experimental studies have already been carried out for various types of F-AF systems including F-AF alloy bilayers. Early references may be found in the review article by Yelon.[2] More recent developments are discussed in the article by Herman and Lambin.[3] During the past few years, F-AF systems such as FeNi/FeMn bilayers[4-6] and Co/Cr multilayers[7-9] have been extensively investigated experimentally as well as theoretically. The quality of experimental samples has greatly improved recently thanks to technical advances in the growth and characterization of magnetic thin films.

On the theoretical side, the magnetic properties of F-AF systems have been studied in terms of the localized-spin and the itinerant-electron models. According to the localized-spin approach, a F-AF bilayer is represented by a Heisenberg or Ising model, and each F (AF) layer is assigned a magnetic moment M_f (M_a). Let us denote the thickness of the F (AF) region by N_f (N_a). One now introduces the unidirectional exchange anisotropy

$$H_{ud}=\mathcal{J}\cos\theta \ , \tag{1.1}$$

where $\mathcal{J}$ is the exchange anisotropy constant and θ denotes the angle between the magnetic moments at the F-AF interface. Note that this expression is quite different from the uniaxial crystalline anisotropy

$$H_{ua}=K\cos^2\theta' \ , \tag{1.2}$$

where K is the crystalline anisotropy constant and θ' is the angle between magnetization and the z axis. The source of the exchange anisotropy is the uncompensated antiferromagnetic moments near the F-AF interfaces, while that of the crystalline anisotropy is the spin-orbit interaction.[1,2] One of the manifestations of the effective anisotropy is a shift of the B-H curve, conventionally referred to as the effective exchange field, H_{ex}. This shift is given by[1,2]

$$H_{ex}=\frac{\mathcal{J}}{M_f N_f} \ , \tag{1.3}$$

with

$$\mathcal{J}=JM_f M_a \ , \tag{1.4}$$

where J is the nearest-neighbor exchange interaction across the F-AF interface. If we evaluate H_{ex} from Eqs. (1.3) and (1.4), assuming J to be the same as that in a F layer, the calculated H_{ex} is larger by orders of magnitude than the observed value. The origin of this discrepancy has been attributed to various physical factors, including the presence of atomic roughness[4,5] and domain walls[6] at the interface. It is well known that both $\mathcal{J}$ and H_{ex} have a characteristic temperature dependence, namely, an almost linear decrease up to the critical temperature.[2] Tsang *et al.*[4] tried to explain this behavior by employing a model which assumes that the interface can be characterized by an ensemble of ordering temperatures having a Gaussian distribution.

Since most F-AF interfaces are composed of transition metals, it is more natural to study their magnetic properties in terms of the itinerant rather than the localized-spin model. Furthermore, because the physical origin of exchange anisotropy, whatever this might be in particular

systems, is undoubtedly localized near the interfaces, it is important to take into account modifications in electronic and magnetic properties near the interface to ensure a proper description of the exchange anisotropy. Such interfacial magnetic problems have already been investigated within the framework of first-principles band calculations based on the local-spin-density-functional (LSDF) method for various multilayer systesm. For example, Lambin and Herman[3] and Herman *et al.*[10] carried out detailed calculations for FeMn/FeNi and Co/Cr multilayers. They succeeded in obtaining the spatial distribution of the local magnetic moments in these multilayers, but they neglected crystalline anisotropy and confined their studies to ground-state (zero-temperature) properties.

In the last decade, there have been significant developments in the theory of finite-temperature band magnetism.[11] As a result, we are now able to discuss the magnetic properties of transition metals at finite temperatures within the itinerant model. Hubbard[12] and Hasegawa[13] independently proposed the single-site spin-fluctuation theory, according to which the effect of spin fluctuations is taken into account by means of the functional integral method within the static approximation. The system under consideration is regarded as a collection of local magnetic moments, and this is treated as a multicomponent alloy by employing the alloy-analogy approximation[14] in conjunction with the coherent potential approximation (CPA). One of the advantages of the single-site spin-fluctuation theory[12,13] is that one can interpolate between the weak- and strong-interaction limits. In the weak-coupling limit, the theory is equivalent to the Hartree-Fock or Stoner theory; in the opposite strong-coupling limit, the theory reduces to the molecular-field Heisenberg model. The finite-temperature band theory[12,13] has proved particularly useful in understanding various finite-temperature properties of bulk,[15,16] surface,[17] and thin-film[18] transition-metal systems.

In a previous paper[19] (referred to as I hereafter), we considered the Co/Cr superlattice as a prototype F-AF interface system. In I we treat the simplest, computationally tractable ultrathin four-layer (1 Co + 3 Cr) superlattice using a suitably parametrized tight-binding band-structure model. The finite-temperature properties of this hypothetical Co/Cr bilayer were studied by using the spin-fluctuation theory.[12,13] Although we expect this ultrathin film to exhibit the essential features of more general Co/Cr superlattices, we felt it was important to verify this point by treating more realistic, thicker multilayer systems, this being one of the principal purposes of the present paper. Accordingly, we will now investigate in some detail a larger eight-layer (3 Co + 5 Cr) superlattice, again studying its finite-temperature magnetic properties by employing the single-site spin-fluctuation theory of Hubbard[12] and Hasegawa.[13] We will also carry out related calculations for Co/Cr superlattices having a wide range of Co and Cr thicknesses so as to provide further evidence for the generality of our results.

The second purpose of this paper is to calculate other important magnetic properties within the framework of itinerant-electron theory. In particular, we will examine the temperature dependence of the exchange anisotropy constant, $\mathcal{J}$, the effective exchange field, H_{ex}, and the nearest-neighbor exchange interactions in the Co/Cr superlattice. To the best of our knowledge, this is the first microscopic calculation of $\mathcal{J}$ and H_{ex} for a F-AF interfacial system. These extended results help us understand the peculiar temperature dependence of the interfacial Cr magnetic moments and of the exchange anisotropy constants.

The paper is organized as follows: In Sec. II we describe the model and the essential features of calculational method. We also briefly review the single-site spin-fluctuation theory. In Sec. III we discuss the calculated magnetic moments and electronic densities of states. In Sec. IV we discuss the temperature dependence of the exchange anisotropy constant and of the effective exchange field. In Sec. V we discuss our approximations further, and in Sec. VI we summarize our conclusions.

II. THEORETICAL MODEL AND METHOD OF CALCULATION

We adopt an eight-layer (3 Co + 5 Cr) Co/Cr superlattice, in which both Co and Cr atoms are assumed to lie on a common bcc lattice with [001] interface. All atoms in a given layer are assumed to have the same magnetic moment. The layers parallel to the interface are denoted by the index n, which runs from 1 to 8. We neglect the small mismatch (about 2%) of the lattice constants as well as the crystalline anisotropy in order to simplify our calculations (see also Sec. V). For this magnetic superlattice, we employ the model Hamiltonian given by

$$H=H_0+H_I \ , \tag{2.1}$$

where H_0 and H_I denote the one-electron and interaction terms, respectively. The one-electron term is expressed by the tight-binding d-band Hamiltonian as

$$H_0=\sum_{\sigma}\sum_{j}\sum_{m}E_j a^{\dagger}_{jm\sigma}a_{jm\sigma}+\sum_{\sigma}\sum_{j,j'}\sum_{m,m'}t^{mm'}_{jj'}a^{\dagger}_{jm\sigma}a_{j'm'\sigma} \ , \tag{2.2}$$

where $a^{\dagger}_{jm\sigma}$ ($a_{jm\sigma}$) is a creation (annihilation) operator of a σ-spin electron of the orbital m on the lattice site j. The core potential, E_j, is assumed to be common for all orbitals and the two-center transfer integrals, $t^{mm'}_{jj'}$, are given by the canonical relation[20]

$$\left.\begin{matrix}(dd\sigma)\\(dd\pi)\\(dd\delta)\end{matrix}\right\}=\left\{\begin{matrix}-6\\4\\-1\end{matrix}\right\}\times(W_d/2.5)(S/R)^5 \ , \tag{2.3a}$$
$$\tag{2.3b}$$
$$\tag{2.3c}$$

where R is the interatomic distance, $S=(3/16\pi)^{1/3}a$ is the Wigner-Seitz radius, a is the bcc lattice constant, and W_d is the bandwidth parameter.[20] For W_d we use the values of 5.44 and 8.00 eV for Co and Cr, respectively, as given by canonical band theory.[20] As for the transfer integrals between Co/Cr pairs, we assume the geometrical average of the values of Co-Co and Cr-Cr pairs.[20]

The interaction term in Eq. (2.1) is given by

$$H_I=(\tfrac{1}{4})\sum_j(U_jN_j^2-J_jM_j^2) \ , \tag{2.4}$$

where N_j (M_j) denotes the total charge (magnetic-moment) operator at the site j, and U_j and J_j are Coulomb and exchange interactions, respectively.[21]

For a study of the finite-temperature magnetism of Co/Cr superlattices, we adopt the single-site spin-fluctuation theory proposed by Hubbard[12] and Hasegawa.[13] When we apply the functional-integral method to the model Hamiltonian given by Eqs. (2.1), (2.2), and (2.4), the partition function, Z, is given within the static approximation by[12,13]

$$Z \sim \int \prod_j d\nu_j \prod_j d\zeta_j \exp[-\beta(\phi_0+\phi_1)] , \tag{2.5}$$

with

$$\phi_0=(\tfrac{1}{4})\sum_j (U_j\nu_j^2+J_j\zeta_j^2) , \tag{2.6}$$

$$\exp(-\beta\phi_1)=\mathrm{Tr}\exp(-\beta H_{\mathrm{eff}}) , \tag{2.7}$$

and

$$H_{\mathrm{eff}}=\sum_j [(E_j-\tfrac{1}{2}iU_j\nu_j)N_j-\tfrac{1}{2}J_j\zeta_j M_j]+H_0^t , \tag{2.8}$$

where H_0^t denotes the hopping term in Eq. (2.2). Equations (2.5)–(2.8) show that the partition function of the interacting system given by Eqs. (2.1)–(2.4) can be evaluated by calculating the partition function of the effective one-electron system given by H_{eff}, including the random charge (ν_j) and exchange (ζ_j) fields. The former field is included by the saddle-point approximation, and the latter is taken into account by the alloy-analogy approximation[14] together with the coherent potential approximation. The self-consistent equations for the average of the exchange field, $\langle\zeta\rangle_n$, its amplitude, $\langle\zeta^2\rangle_n$, and the number of electrons on layer n, $\langle n\rangle_n$, are given by

$$\langle\zeta\rangle_n=\int d\zeta_j\,\zeta_j C_n(\zeta_j) , \tag{2.9}$$

$$\langle\zeta^2\rangle_n=\int d\zeta_j\,\zeta_j^2 C_n(\zeta_j) , \tag{2.10}$$

and

$$\langle n\rangle_n=\int d\varepsilon\, f(\varepsilon)(-1/\pi)\mathrm{Im}\sum_\sigma F_{n\sigma}(\varepsilon) . \tag{2.11}$$

In Eqs. (2.9) and (2.10), $C_n(\zeta_j)$ denotes the distribution of the potential of $\sigma(J_n/2)\zeta_j$ at the site j on the layer n and it is given by

$$C_n(\zeta_j)=\{\exp[-\beta\psi_n(\zeta_j)]\}/\int d\zeta_j\exp[-\beta\psi_n(\zeta_j)] , \tag{2.12}$$

with

$$\psi_n(\zeta_j)=(J_n/4)\zeta_j^2-(U_n/4)\langle n(\zeta_j)\rangle_n^2+\int d\varepsilon\, f(\varepsilon)(1/\pi)\sum_\sigma \mathrm{Im}\ln[1-V_{n\sigma}(\varepsilon)F_{n\sigma}(\varepsilon)] , \tag{2.13}$$

$$\langle n(\zeta_j)\rangle_n=\int d\varepsilon\, f(\varepsilon)(-1/\pi)\sum_\sigma \mathrm{Im}\{F_{n\sigma}(\varepsilon)/[1-V_{n\sigma}(\varepsilon)F_{n\sigma}(\varepsilon)]\} , \tag{2.14}$$

$$V_{n\sigma}(\varepsilon)=E_n+(U_n/2)\langle n(\zeta_j)\rangle_n-\sigma(J_n/2)\zeta_j-\Sigma_{n\sigma}(\varepsilon) , \tag{2.15}$$

$$\tilde{\Sigma}_{n\sigma}(\varepsilon)\equiv\Sigma_{n\sigma}(\varepsilon)-E_n-(U_n/2)\langle n\rangle_n=-\sigma(J_n/2)\langle\zeta\rangle_n+[(J_n^2/4)\langle\zeta^2\rangle_n-\tilde{\Sigma}_{n\sigma}^2(\varepsilon)]F_{n\sigma}(\varepsilon) . \tag{2.16}$$

The local Green function, $F_{n\sigma}(\varepsilon)$, and the coherent potential, $\Sigma_{n\sigma}(\varepsilon)$, of an electron with spin σ on the layer n are calculated by solving the CPA equation given by Eq. (2.16) using the generalized "transfer-matrix method."[17]

The Fermi-distribution function, $f(\varepsilon)$, is included with the use of the contour integral along the complex energy axis.[17] This makes it easier to solve the CPA equation and to get $F_{n\sigma}(\varepsilon)$ with a fairly small number of sampling points (15) in the irreducible part of the [001] bcc surface Brillouin zone. After the self-consistent equations given by Eqs. (2.9)–(2.16) are solved by an iterative method, we calculate the average magnetic moment on site n and its root-mean-square (rms) value by

$$\langle M\rangle_n=5\langle\zeta\rangle_n , \tag{2.17}$$

$$\langle M^2\rangle_n^{1/2}=5[\langle\zeta^2\rangle_n-(\tfrac{2}{5})(T/J_n)]^{1/2} , \tag{2.18}$$

where the factor 5 denotes the orbital degeneracy of d bands. The total magnetic moment per atom is defined by

$$\langle M\rangle=(\tfrac{1}{8})\sum_n\langle M\rangle_n . \tag{2.19}$$

The local density of states on the nth layer of σ electrons, $\rho_{n\sigma}(\varepsilon)$, which will be shown in Sec. III, is given by

$$\rho_{n\sigma}(\varepsilon)=(-1/\pi)\mathrm{Im}F_{n\sigma}(\varepsilon+i\delta) \tag{2.20}$$

with an imaginary part of $\delta=0.05$ eV.

III. CALCULATED MAGNETIC PROPERTIES

A. Ground state

Let us first discuss the parameters E_n, W_d, U_n, and J_n adopted in our calculation. In I,[19] we determined these parameters so that our ground-state calculation for a four-layer (1 Co + 3 Cr) superlattice faithfully reproduced the corresponding result obtained by a detailed band calculation using the LSDF method[10] (cf. I, Fig. 1). In the present calculation, we employ the same parameters as in I. These parameters are listed in Table I, where

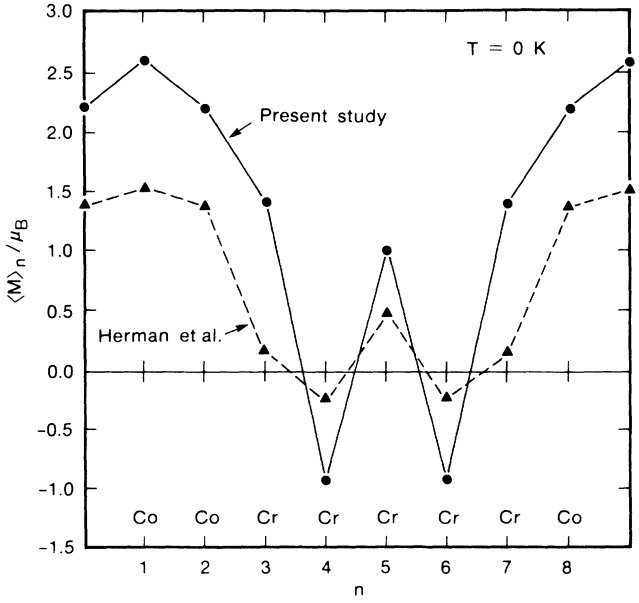

FIG. 1. The distribution of local magnetic moments at $T=0$ K in 3 Co + 5 Cr superlattices as given by our calculation (solid curves) and by Herman and Lambin (dashed curves, Ref. 10).

we assume $U_n = J_n$. The parameters shown in Table I lead to the ferromagnetic ground state in bulk Co with magnetic moment of $1.7\mu_B$ and the commensurate antiferromagnetic state in bulk Cr with sublattice magnetic moment of $0.6\mu_B$.[17] Our Co result is consistent with experiment[7] and with the LSDF band calculations for bcc Co.[22,23] Bearing in mind that our Cr result refers to a commensurate antiferromagnetic phase, it compares favorably with the observed maximum value of the spin-density wave (SDW) of $0.59\mu_B$.[24] Our Cr result is also consistent with the results of some recent band calculations[25,26] for commensurate antiferromagnetic Cr, although smaller sublattice moments were reported in other band calculations.[27,28]

The calculated moment distribution in the 3 Co + 5 Cr superlattice is shown in Fig. 1, where for comparison we also plot the corresponding quantities given by the detailed band calculations of Herman *et al.*[10] Although the results of these two calculations are somewhat different in detail, the general trend of the first-principles results is reasonably well reproduced by our simple tight-binding model. We could have adjusted our parameters to obtain closer agreement between the two sets of calculations, but the possibility of comparing our results for different superlattice geometries using the same parameters outweighed the nominal advantages of carrying out such an adjustment. In any event, the differences already mentioned are not unexpected, since self-consistent charge redistributions are taken into account in the first-principles calculations but not in the tight-binding models.

Although relevant experimental data are not available at the moment with which to test our theoretical results, it is anticipated that such data will become available in due course as molecular-beam-epitaxy (MBE) techniques continue to improve. Two of our experimental colleagues, Dr. Robin Farrow and Dr. Stuart Parkin, are currently attempting to grow ultrathin ferromagnetic-antiferromagnetic interfaces by MBE.

In Fig. 1 we note that magnetic moments on Cr layers alternate from layer to layer and Co moments couple ferromagnetically across the Co/Cr interfaces. We found an alternative antiferromagnetic solution across the interface, just as was found earlier in the detailed band calculation.[10] However, this antiferromagnetic solution was estimated to be unstable compared to the ferromagnetic solution and, hence, was disregarded.

The ground-state local density of states on each layer is shown in Fig. 2. The density of states on the central Co layer [Co(1)] is almost the same as that of bcc Fe: Note that the magnetic moment of the central Co of $2.6\mu_B$ is comparable to $2.2\mu_B$ in bcc Fe. Similarly, the densities of states on the central Cr [Cr(5)] and subinterface Cr [Cr(4)] layers are almost the same as that for pure Cr. In contrast, the densities of states on interfacial Co [Co(2)]

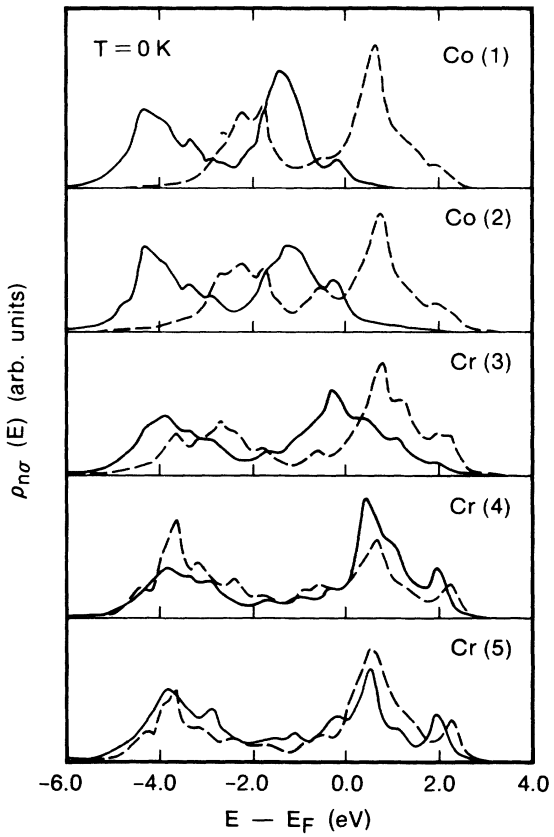

FIG. 2. The ground-state local densities of states, $\rho_{n\sigma}(\varepsilon)$, the solid (dashed) curves denoting the up-spin (down-spin) component. Numbers in parentheses express layer indices, n. From the symmetry, Cr(6), Cr(7), and Co(8) are equivalent to Cr(4), Cr(3), and Co(2), respectively.

TABLE I. Band structure parameters (in eV).

Atom	E_n	W_d	U_n
Cr	0.00	8.00	0.67
Co	−1.40	5.44	0.80

and Cr [Cr(3)] layers are different from those of bulk Co and Cr layers. In particular, the density of states on the interfacial Cr [Cr(3)] layer is modified appreciably because of the presence of the nearby strongly ferromagnetic Co layer.

B. Finite temperatures

The temperature dependence of the average magnetic moment on each layer in the 3 Co + 5 Cr superlattice is shown in Fig. 3. The $\langle M \rangle_n$ curve of the central Co [Co(1)] approximately follows the Brillouin function for $S=\frac{1}{2}$. On the other hand, the $\langle M \rangle_n$ curves for the Cr layers show a very peculiar temperature dependence. This can be understood as due to a fairly weak magnetic coupling across the interfacial Co/Cr layers, as we will discuss in more detail later. The $\langle M \rangle_n$ curve of the interface Co [Co(2)] deviates slightly downwards from the Brillouin function, being influenced by Cr layers. The calculated Curie temperature of 3 Co + 5 Cr superlattice is 3000 K while that of 1 Co + 3 Cr is 1600 K.[19] We plot in Fig. 4 the Curie temperature of p Co-$(p+2)$ Cr superlattices as a function p; the 1 Co + 3 Cr and 3 Co + 5 Cr superlattices correspond to $p=1$ and 3, respectively. We also include the results for pure Cr as a special case of $p=0$. Judging from the fact that the observed Curie temperature of pure fcc Co is 1400 K, the calculated Curie temperatures are expected to be overestimated. This is due to the neglect of the magnetic short-range order and the dynamical effect of spin fluctuations in our spin-fluctuation theory.[12,13] Nevertheless, the calculated trend showing higher T_C for larger p is reasonable because the strong magnetic interactions of Co atoms are expected to work to elevate the Curie temperature.

In Fig. 5 we display the temperature dependence of the total magnetic moment, which also shows a deviation from the Brillouin function.

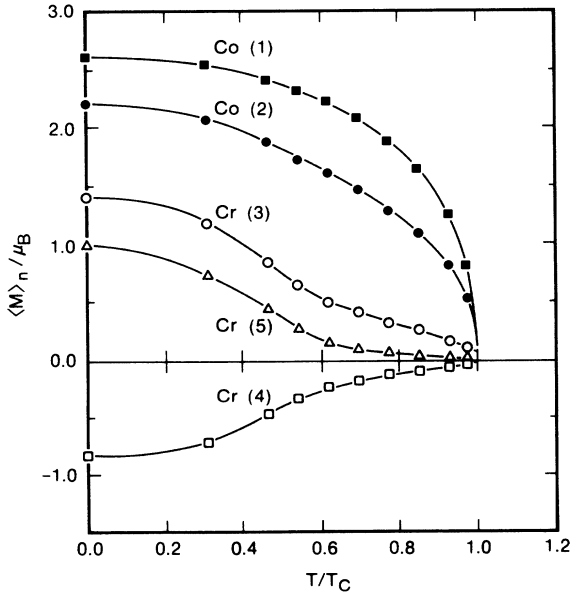

FIG. 3. The temperature dependence of the average magnetic moment on the nth layer, $\langle M \rangle_n$.

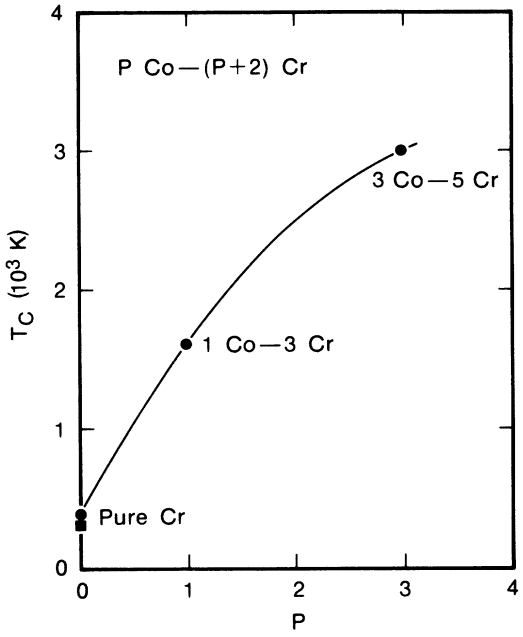

FIG. 4. The Curie temperature, T_C, of the p Co + $(p+2)$ Cr superlattice as a function of p. Calculated (●) and observed (■) results for pure Cr are shown by $p=0$.

The temperature dependence of the rms value of local moments is plotted in Fig. 6. We note that the amplitudes of local moments is almost temperature independent and persists above the Curie temperature, T_C.

The temperature dependence of the local densities of states on Co and Cr layers is shown in Figs. 7 and 8, respectively. When the temperature is raised, the shape of the densities of states becomes obscure because of the random local moments. The temperature dependence of local densities of states on the central Co [cf. Fig. 7(a)] and Cr [cf. Fig. 8(a)] are nearly the same as those of bulk Fe and Cr, respectively.[17]

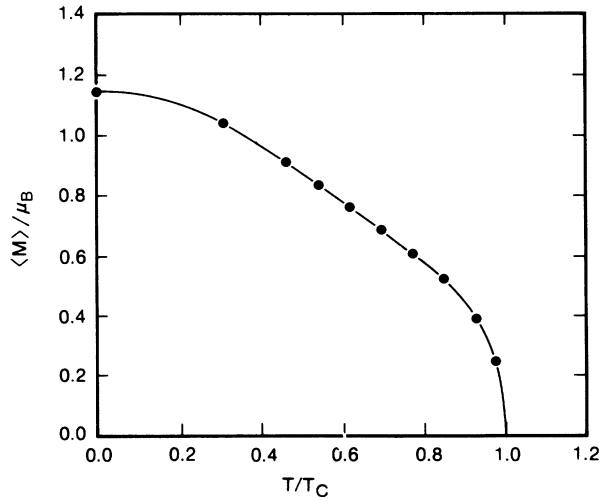

FIG. 5. The temperature dependence of the total magnetic moment per atom, $\langle M \rangle$.

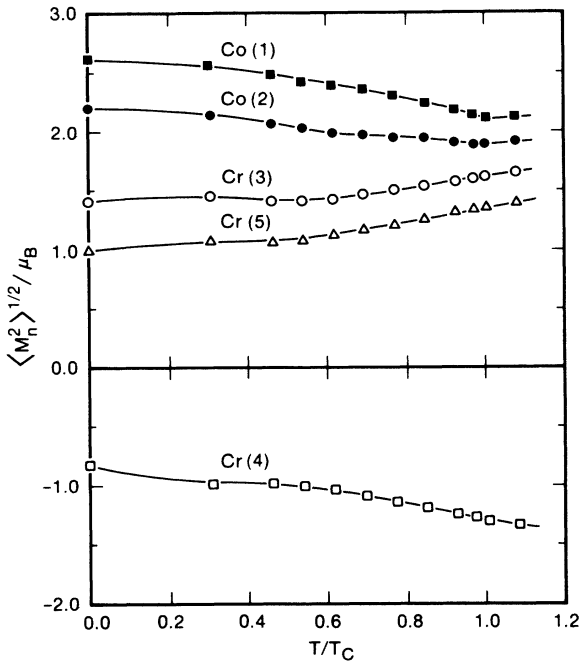

FIG. 6. The temperature dependence of the rms value of magnetic moments on the nth layer, $\langle M^2 \rangle_n^{1/2}$.

IV. EXCHANGE ANISOTROPY CONSTANT AND EFFECTIVE EXCHANGE FIELD

We will calculate the temperature dependence of the exchange anisotropy constant, $\mathcal{J}$, and of the effective exchange field, H_{ex}, by considering a shift in the B-H curve [cf. Fig. 9(a)]. In order to simplify our calculation, we adopt the following approximations.

(1) We neglect the crystalline anisotropy in the F layers.

(2) The crystalline anisotropy in the AF layers, which is indispensable for a calculation of $\mathcal{J}$ and H_{ex}, is *implicitly* taken into account by assuming fixed AF magnetic moments.

(3) H_{ex} and $(J_n/2)\langle M \rangle_n$ are assumed to be small compared to the characteristic band energy.

The first approximation leads to a B-H curve with vanishing coercivity, H_c, because its main origin is known to be the crystalline anisotropy in the F layers. Thus, the transition in our superlattice is assumed to occur at H_{ex} from the point X to the point Y in Fig. 9(b). The second approximaton assumes that only the direction of magnetic moments in F layers is reversed at the transition from points X to Y, while magnetic moments in AF layers remain unchanged [cf. Figs. 9(c) and (d)]. The effective exchange field, H_{ex}, is determined by the condition

$$F_X(H_{ex},T)=F_Y(H_{ex},T)\ , \tag{4.1a}$$

where

$$F_X(H,T)=-\beta^{-1}\ln Z_X(H,T) \tag{4.1b}$$

denotes the free energy of the system with the spin configuration X under the applied magnetic field H at temperature T. By using assumption (3), we expand the free energy in terms of H_{ex} and $\langle M \rangle_n$ to get

$$H_{ex}\sum_{n\in F}\langle M \rangle_n=\sum_{n\in F}\sum_{n'\in AF}\mathcal{J}_{nn'}\langle M \rangle_n\langle M \rangle_{n'}\ , \tag{4.2}$$

where $\mathcal{J}_{nn'}$ stands for the interlayer exchange interaction between the magnetic moments on n and n' layers given by

$$\mathcal{J}_{nn'}=J_nJ_{n'}\int d\varepsilon\, f(\varepsilon)\sum_{\sigma}(1/\pi)\mathrm{Im}(\eta_{n\sigma}\eta_{n'\sigma}\mathrm{Tr}G_{nn'\sigma}G_{n'n\sigma})\ , \tag{4.3}$$

$$\eta_{n\sigma}=\{1+[\tilde{\Sigma}_{n\sigma}+\sigma(J_n/2)\langle M \rangle_n]F_{n\sigma}\}^{-1}\ . \tag{4.4}$$

In Eqs. (4.3) and (4.4), Tr stands for the trace over the orbitals, $G_{nn'\sigma}$ is the Green-function matrix, and $\tilde{\Sigma}_{n\sigma}$ denotes the coherent potential for electrons on the layer n

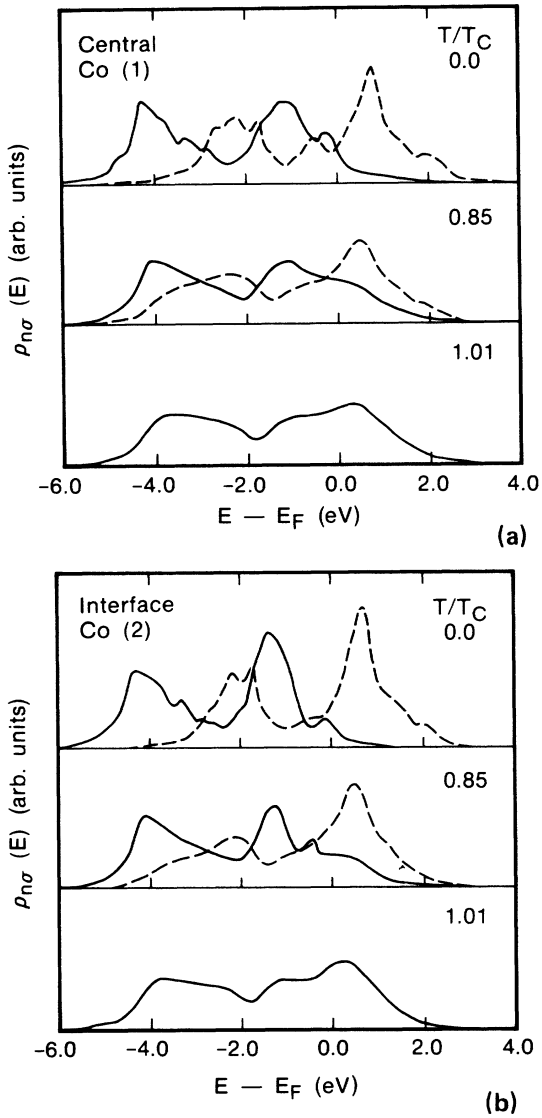

FIG. 7. The temperature dependence of Co densities of states on (a) central [Co(1)] and (b) interface [Co(2)] layers, the solid (dashed) curves denoting the up-spin (down-spin) component.

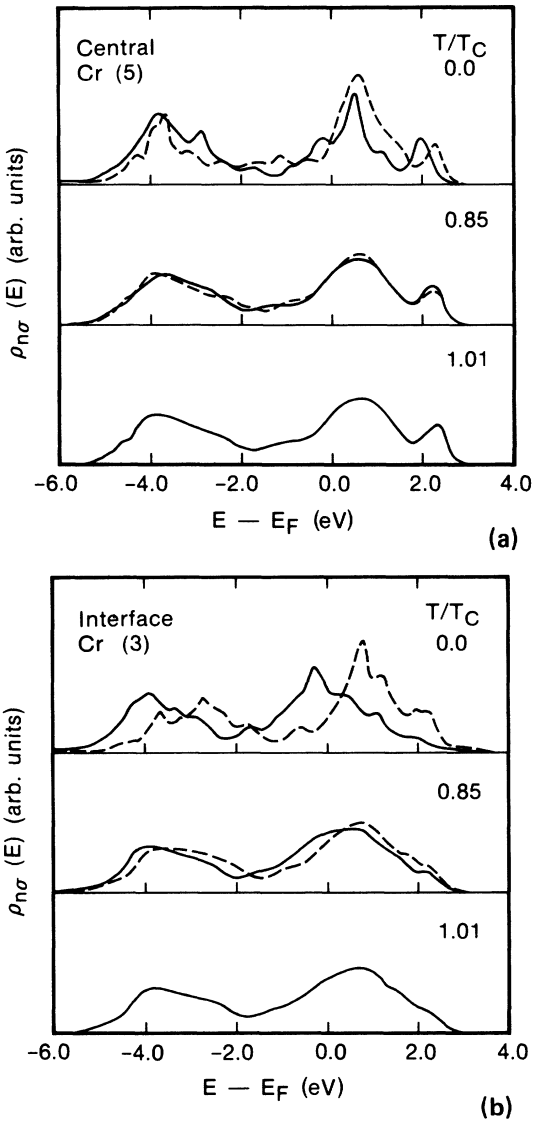

FIG. 8. The temperature dependence of Cr densities of states on (a) central [Cr(5)] and (b) interface [Cr(3)] layers, the solid (dashed) curves denoting the up-spin (down-spin) component.

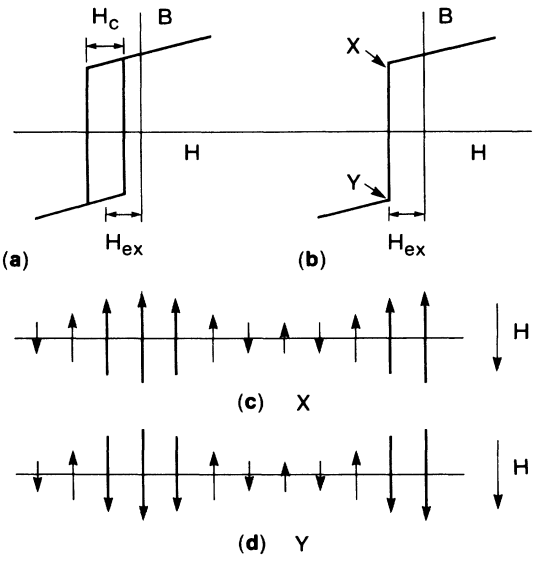

FIG. 9. Schematic figures of the B-H curves shifted by H_{ex} (a) with and (b) without the coercivity, H_c. Assumed distributions of magnetic moments on Co layers (bold lines) and Cr layers (thin lines) at the (c) X and (d) Y points are described (see text).

with spin σ given by Eq. (2.16). The left-hand side of Eq. (4.2) expresses the Zeeman-energy gain in the F layers under the applied magnetic field, H_{ex}, whereas the right-hand side denotes the energy gain in the F layers due to the exchange field arising from the AF layers through the interaction, $\mathcal{J}_{nn'}$. When the nearest-neighbor interactions are predominant, Eq. (4.2) leads to[29]

$$H_{ex}=\frac{2\mathcal{J}}{\sum_{n\in F}\langle M\rangle_n}\ , \tag{4.5}$$

with

$$\mathcal{J}=\mathcal{J}_{\mathrm{CoI,CrI}}\langle M\rangle_{\mathrm{CoI}}\langle M\rangle_{\mathrm{CrI}}\ , \tag{4.6}$$

where $\mathcal{J}_{\mathrm{CoI,CrI}}$ is the interlayer exchange interaction across the Co/Cr interfaces and $\langle M\rangle_{\mathrm{CoI}}(\langle M\rangle_{\mathrm{CrI}})$ is the magnetic moment on the interface Co (Cr) layer. It should be noted that when magnitudes of moments are uniform (i.e., $\langle M\rangle_n=M_f$), Eq. (4.5) reduces to

$$H_{ex}=\frac{2\mathcal{J}}{M_f N_f}\ , \tag{4.7}$$

which is nothing but the result obtained using the localized model [cf. Eq. (1.3)].[29]

In order to obtain $\mathcal{J}$ and H_{ex} from Eqs. (4.5) and (4.6), we calculated the nearest-neighbor interlayer interaction, $\mathcal{J}_{nn'}$, in the 3 Co + 5 Cr superlattice; the ground-state results are plotted in Fig. 10. For comparison, the results for pure (bulk) Co and Cr are shown by the arrows along the left abscissa.[30] The calculated value of 0.018 eV for bulk (bcc) Co is similar to 0.026 eV for bcc Fe obtained

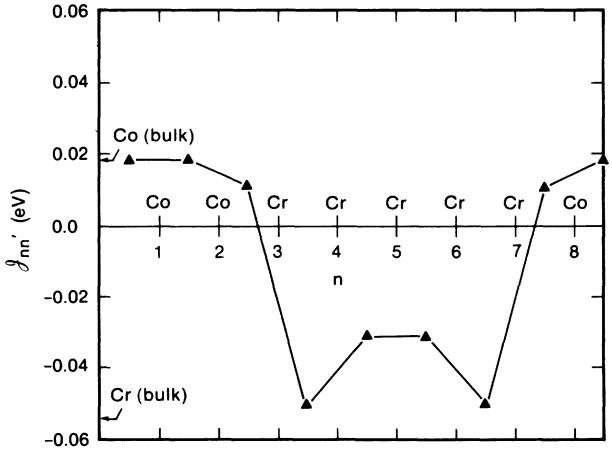

FIG. 10. The nearest-neighbor interlayer exchange interaction, $\mathcal{J}_{nn'}$, at $T=0$ K in 3 Co + 5 Cr superlattices, the arrows denoting the results for bulk Co and Cr.

by Hubbard.[12] The sign of $\mathcal{J}_{nn'}$ for a Co-Co pair is positive while that for a Cr-Cr pair is negative, as we might expect. We note that, although $\mathcal{J}_{nn'}$ for the interfacial Co/Cr pair is positive, its magnitude is much smaller than that of Co-Co pairs. This is realized also at finite temperatures, as shown in Fig. 11, where the $\mathcal{J}_{nn'}$ are plotted as a function of the temperature.

This small interfacial interaction is the origin of the peculiar temperature dependence of the Cr moments (cf. Fig. 3). We should note that if the interfacial interaction is vanishing ($\mathcal{J}_{nn'}=0$), Co and Cr layers have two distinct transition temperatures of T_C(Co) and T_N(Cr), the former being expected to be larger than the latter. When a small interaction is introduced into the Co/Cr interface, the Cr layers near the Co/Cr interface can be polarized even at $T_N(\mathrm{Cr}) < T < T_C(\mathrm{Co})$ because of the exchange field arising from Co layers through the weak $\mathcal{J}_{nn'}$. This yields peculiarly temperature-dependent Cr moments, as was shown in Fig. 3.

Figure 12 shows the temperature dependence of $\mathcal{J}$ and H_{ex} which are calculated by using Eqs. (4.5) and (4.6). We note an unusual temperature dependence of $\mathcal{J}$ and H_{ex}, both deviating significantly from the Brillouin function and showing an almost linear temperature dependence at $T/T_C \gtrsim 0.5$. This is mainly due to the peculiar temperature dependence of Cr moments near the Co/Cr interfaces, and this feature is widely observed in many F-AF interface systems.[2] Our calculation shows a peak in $\mathcal{J}$ (and H_{ex}) at $T/T_C \sim 0.3$, which arises from the combined effects of an increase in $\mathcal{J}_{\mathrm{CoI,CrI}}$ (cf. Fig. 11) and a decrease in Cr moments (cf. Fig. 3) when the temperature is raised. The presence of such peaks was reported in some F-AF systems, for example, $Ni_{0.81}Fe_{0.19}/Mn$,[31] but not in others such as MnFe/NiFe.[4] The absence of the peaks would be realized if both the interlayer exchange interaction and the interfacial moment decrease monotonically when the temperature is raised.

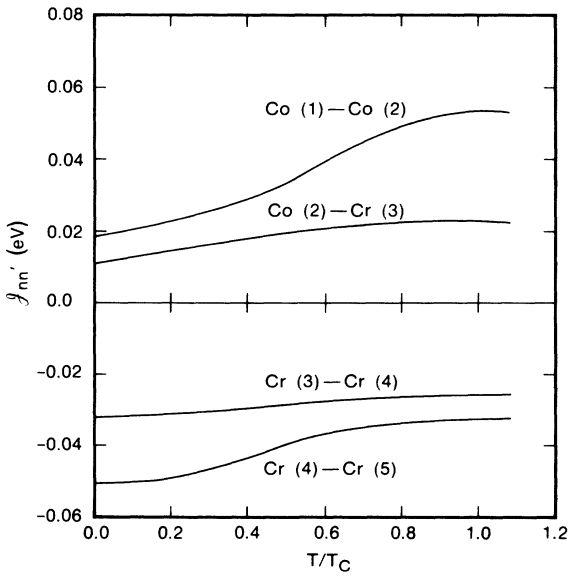

FIG. 11. The temperature dependence of the nearest-neighbor interlayer exchange interaction, $\mathcal{J}_{nn'}$.

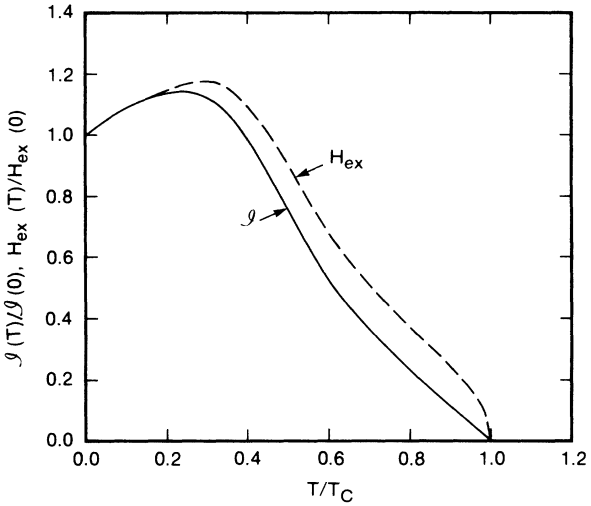

FIG. 12. The temperature dependence of the exchange anisotropy constant, $\mathcal{J}$ (solid curve), and the effective exchange field, H_{ex} (dashed curve).

The calculated anisotropy constant at $T=0$ K, $\mathcal{J}(0)$, is 0.033 eV$=5.3\times10^{-14}$ ergs, which is given by $\mathcal{J}_{\mathrm{CoI,CrI}}=0.011$ eV$=1.7\times10^{-14}$ ergs, $\langle M\rangle_{\mathrm{CoI}}=2.2\mu_B$, and $\langle M\rangle_{\mathrm{CrI}}=1.4\mu_B$ in Eq. (4.6). Unfortunately, relevant experimental data for Co/Cr bilayers have not been reported yet. It was shown[5] that in FeMn/FeNi bilayers, the interface interaction, $\mathcal{J}_{nn'}$, deduced from the observed H_{ex} is of order 10^{-16} ergs. This quantitative difference might be due to atomic-scale roughness near the interfaces[4,5] and/or domain walls,[6] which might exist in real systems but are not included in this calculation.

V. DISCUSSION

In judging the significance of our results, it is necessary to examine the approximations which have been introduced in our calculation. The static approximation for the functional-integral method neglects the effect of dynamical spin fluctuations such as spin waves. This is one of the reasons that this approach overestimates Curie temperatures. It also leads to the absence of the $\frac{3}{2}$-power law in the temperature dependence of $\langle M\rangle_n$ at low temperatures. Several authors[32] investigated spin waves in F-AF superlattices, and demonstrated that these have properties distinctly different from those in bulk systems. These studies are, however, based on the localized model[32] and no calculations have been reported so far using the itinerant model.

A more serious approximation is the neglect of the crystalline anisotropy. Calculations using the localized model have shown that the effect of crystalline anisotropy plays an important role in determining the low-temperature magnetic properties of surface-related systems[33] and also the B-H curve of the F-AF interfaces.[34] Quite recently, the ground-state anisotropy constants of unsupported transition-metal thin films were calculated by a first-principles method by incorporating the spin-

orbit interaction.[35] It was shown that the crystalline anisotropy constant of a Fe monolayer is about 100 times larger than that of bulk Fe.[35,36] This is a consequence of the reduced symmetry of isolated monolayers, which introduces anisotropy in second rather than fourth order (for cubic crystals).

These remarks suggest that the anisotropy in multilayers should be much smaller than that of unsupported thin films because the atoms in the former have neighboring atoms in three dimensions rather than in only two dimensions. To some extent, these symmetry and dimensional arguments justify our neglect of crystalline anisotropy. We can include the effect of crystalline anisotropy phenomenologically in a variety of ways, for example, by introducing an anisotropy field in the Hubbard Hamiltonian. However, it is very difficult to treat the temperature dependence of the anisotropy constants even in a phenomenological way, because they are reported to show a rather unusual temperature dependence.[37] The microscopic calculation of the temperature dependence of the crystalline anisotropy constants remains a challenging subject for future studies.

VI. CONCLUSIONS

Using the Hubbard-Hasegawa theory,[12,13] we examined the finite-temperature magnetic properties of Co/Cr superlattices. We also calculated the temperature dependence of the exchange anisotropy constant, $\mathcal{J}$, and of the effective exchange field, H_{ex}. One of the important results obtained in our calculation is a fairly small interlayer exchange interaction across the Co/Cr interface. This result can be inferred from the peculiar temperature dependence of magnetic moments near the interfaces (cf. Fig. 3; see also I, Fig. 2), and can be demonstrated explictly by direct calculation of the nearest-neighbor interlayer exchange interaction $\mathcal{J}_{nn'}$ (cf. Figs. 10 and 11). It is possible that this small interlayer exchange interaction across the F-AF interface is a common feature of F-AF interface systems. In fact, we obtained the same results in a preliminary calculation for FeMn/FeNi bilayers.[38] The characteristic temperature dependence of $\mathcal{J}$ and H_{ex} observed in many F-AF interface systems[2] is accounted for quite nicely by our calculation without invoking any artificial assumptions (cf. Fig. 12). It would be interesting for experimentalists to prepare ultrathin Co/Cr superlattices of the type treated here, and examine the predicted temperature dependence of interfacial magnetic moments and effective exchange fields, so as to check the adequacy of the present theoretical treatment.

Since the exchange anisotropy has a local origin near the F-AF interface, as already emphasized, we believe that the principal conclusions obtained here for the 3 Co + 5 Cr superlattice would remain valid even if the number of Co and Cr layers is increased.[39] More generally, we would expect our simple calculations, the first microscopic calculations based on the itinerant model, to account for the essential features observed in a wide range of F-AF interface systems.

ACKNOWELDGMENTS

The authors wish to express their sincere thanks to Dr. R. Farrow, Dr. D. Mauri, Dr. R. K. Nesbet, Dr. S. S. P. Parkin, Dr. M. Toney, and Dr. C. Tsang for valuable discussions. One of the authors (H.H.) wishes to thank IBM Japan for making it possible for him to spend a year at IBM Almaden Research Center, San Jose. This research was supported in part by the Office of Naval Research.

---

*Permanent address.

[1]W. H. Meiklejohn and C. P. Bean, Phys. Rev. **105**, 904 (1957).

[2]A. Yelon, in *Physics of Thin Films,* edited by M. Fracombe and R. Hoffman (Academic, New York, 1971), Vol. 6, p. 205.

[3]Ph. Lambin and F. Herman, Phys. Rev. B **30**, 6903 (1985). For additional references, see the review: N. H. March, Ph. Lambin, and F. Herman, J. Magn. Magn. Mater. **44**, 1 (1984).

[4]C. Tsang, N. Heiman, and K. Lee, J. Appl. Phys. **52**, 2471 (1981).

[5]A. P. Malozemoff, Phys. Rev. B **35**, 3679 (1987).

[6]D. Mauri, H. C. Siegmann, P. S. Bagus, and E. Kay, J. Appl. Phys. **62**, 3047 (1987).

[7]R. Walsley, J. Thomson, D. Friedman, R. M. White, and T. Geballe, IEEE Trans. Magn. **MAG-19**, 1992 (1983).

[8]M. B. Stearns, C. H. Lee, and S. P. Vernon, J. Magn. Magn. Mater. **54-57**, 791 (1986).

[9]B. L. Ramakrishna, M. B. Stearns, and C. H. Lee, J. Appl. Phys. **61**, 4290 (1987).

[10]F. Herman, Ph. Lambin, and O. Jepsen, Phys. Rev. B **31**, 4394 (1985); J. Appl. Phys. **57**, 3654 (1985). In these studies it was found that, for some geometries, there was only one stable solution, while for others there were two, corresponding to ferromagnetic and antiferromagnetic coupling across the interface. When dual solutions did arise, they were both numerically stable. These authors were not able to establish which was the more stable physically since the difference in their total energies was comparable to numerical uncertainties arising from the atomic sphere approximation.

[11]For recent developments in the theory on band magnetism, see *Electron Correlation and Magnetism in Narrow Band Systems,* edited by T. Moriya (Springer, Berlin, 1981); F. Gautier, in *Magnetism of Metals and Alloys,* edited by M. Cryot (North-Holland, Amsterdam, 1982), p. 1.

[12]J. Hubbard, Phys. Rev. B **19**, 2626 (1979); **20**, 4584 (1979); **23**, 5970 (1981).

[13]H. Hasegawa, J. Phys. Soc. Jpn. **46**, 1504 (1979); **49**, 178 (1980).

[14]M. Cryot, J. Phys. (Paris) **33**, 25 (1972).

[15]For applications to transition-metal magnetism, see H. Hasegawa, J. Phys. Soc. Jpn. **49**, 963 (1980); J. Phys. F **13**, 1915 (1983); Y. Kakehashi, J. Phys. Soc. Jpn. **50**, 2236 (1981); J. Magn. Magn. Mater. **37**, 189 (1983); Phys. Rev. B **32**, 3035 (1985).

[16]Y. Kakehashi and H. Hasegawa, Phys. Rev. B **36**, 4066 (1987); **37**, 7777 (1988).

[17]H. Hasegawa, J. Phys. F **16**, 347 (1986); **16**, 1555 (1986); **17**,

165 (1987).
[18]H. Hasegawa, Surf. Sci. **182**, 591 (1987).
[19]H. Hasegawa and F. Herman, Physica **B149**, 175 (1988).
[20]D. G. Pettifor, J. Phys. F **7**, 613 (1977); (private communication).
[21]J_j in Eq. (2.4) should not be confused with the exchange interaction J in the Heisenberg model given in Eq. (1.4).
[22]D. Bagayoko, A. Ziegler, and J. Callaway, Phys. Rev. B **27**, 704 (1983).
[23]V. L. Moruzzi, P. M. Marcus, K. Schwarz, and P. Mohn, Phys. Rev. B **34**, 1784 (1986); J. Magn. Magn. Mater. **54-57**, 955 (1986).
[24]A. Werner, A. Arrott, and H. Kendrick, Phys. Rev. **155**, 528 (1967).
[25]J. Kübler, J. Magn. Magn. Mater. **20**, 277 (1980).
[26]N. I. Kulikov, M. Alouani, M. A. Khan, and M. V. Magnitskaya, Phys. Rev. B **36**, 929 (1987).
[27]H. L. Skriver, J. Phys. F **11**, 97 (1981).
[28]N. I. Kulikov and E. T. Kulatov, J. Phys. F **12**, 2291 (1982).
[29]The factor 2 in Eqs. (4.5) and (4.7) arises from the fact that the superlattice has two F-AF interfaces at both ends of a F layer [cf. Eq. (1.3)].
[30]When we estimate the critical temperatures of bulk Co and Cr from the calculated nearest-neighbor interactions, $\mathcal{J}_{nn'}$, we get $T_C(\mathrm{Co})=1600$ K and $T_N(\mathrm{Cr})=600$ K, by employing the mean-field-type equation $T_{C,N}=(\frac{1}{3})z\,|\,\mathcal{J}_{nn'}\,|\,\langle M^2\rangle$, z being the coordination number. These results are comparable with the observed data of 1400 K and 340 K for Co and Cr, respectively.
[31]O. Massenet, R. Montmory, and L. Néel, IEEE Trans. Magn. MAG-**1**, 63 (1965).
[32]L. L. Hinchey and D. L. Mills, Phys. Rev. **33**, 3329 (1986), and related references therein.
[33]A. Corciovei, Phys. Rev. **130**, 2223 (1963); J. A. Davis and F. Keffer, J. Appl. Phys. **34**, 1135 (1963).
[34]See, for example, Ref. 6.
[35]J. G. Gay and R. Richter, Phys. Rev. **56**, 2728 (1986); J. Appl. Phys. **61**, 3362 (1987).
[36]N. Mori, T. Ukai, and S. Ohtsuka, J. Magn. Magn. Mater. **31-34**, 43 (1983).
[37]U. Gradmann, J. Magn. Magn. Mater. **54-57**, 733 (1986).
[38]H. Hasegawa and F. Herman (unpublished).
[39]We examined "the size effect" in Co/Cr F-AF superlattices further by employing the Heisenberg model characterized by spins, $S_f=2S_a=1$; exchange interactions, $J_{aa}/J_{ff}\equiv j_a$ and $J_{af}/J_{ff}\equiv j_i$; and layer thicknesses, N_f and N_a. The subscript f (a) denotes F (AF) layers. The temperature dependence of the average moments on all the layers was calculated by mean-field theory for various choices of N_f and N_a. At least for multilayers with comparable size F and AF regions, we found that the behavior of the magnetic moments near the F-AF interfaces was not sensitive to the size of the F and AF regions.